toxics

MDPI

Article

Bioremediation Strategies for Marine Sediments Co-Contaminated with PCBs and PBDEs: Insights into Dehalogenation Dynamics, Microbiome Shifts, and Ecological Risk Evaluation

Miray Kurtoğlu [1], Hatice Eser Ökten [2] and Hale Demirtepe [2,*]

[1] Department of Biotechnology and Bioengineering, Graduate School, İzmir Institute of Technology, Urla, İzmir 35430, Türkiye; kurtoglumiray@gmail.com
[2] Department of Environmental Engineering, Faculty of Engineering, İzmir Institute of Technology, Urla, İzmir 35430, Türkiye; haticeokten@iyte.edu.tr
* Correspondence: haledemirtepe@iyte.edu.tr; Tel.: +90-232-750-6855

Abstract

Anaerobic bioremediation offers a sustainable strategy for managing sediments contaminated with halogenated persistent organic pollutants (POPs). However, the dehalogenation dynamics and associated microbial responses in historically contaminated sediments containing multiple POPs remain poorly understood. This study investigated the chemical, microbial, and ecotoxicological dynamics of marine sediments chronically co-contaminated with polychlorinated biphenyls (PCBs) and polybrominated diphenyl ethers (PBDEs). Microcosms using sediments from a shipbreaking zone (Aliağa, Türkiye) simulated bioaugmentation (using site-derived Chloroflexi-containing consortium), biostimulation (through acetate and micronutrients amendments), and natural attenuation. During a 198-day period of operation, substrate preference was observed across all treatments, with PBDEs serving as the primary electron acceptor before active PCB dehalogenation. Biostimulation and bioaugmentation effectively achieved 44% and 42% ΣPCB and 48% and 35% ΣPBDE mass removal, with corresponding daily dehalogenation rates of 0.00174 and 0.00178 chlorine per biphenyl and 0.00805 and 0.00587 bromine per diphenyl ether, respectively. Shotgun metagenomic analysis revealed a major microbial shift from Pseudomonadota to diverse anaerobic communities, with Chloroflexota increasing to 3.0%. While active treatments successfully degraded highly halogenated homologs, the sequential formation and accumulation of lower-halogenated homologs (e.g., mono-CBs, PCB-18, PCB-28, and PCB-52) temporarily increased localized ecological risk quotients. Our findings demonstrate that achieving complete detoxification requires coupling anaerobic dehalogenation with other remediation strategies as polishing stages.

Keywords: anaerobic dehalogenation; ecological risk; marine sediment; microcosm; persistent organic pollutants

Academic Editor: Xiaoshan Zhu

Received: 2 November 2026
Revised: 22 November 2026
Accepted: 26 November 2026
Published: 28 November 2026

Copyright: © 2026 by the authors. Licensee MDPI, Basel, Switzerland. This article is an open access article distributed under the terms and conditions of the Creative Commons Attribution (CC BY) license.

1. Introduction

Persistent organic pollutants (POPs), including polychlorinated biphenyls (PCBs) and polybrominated diphenyl ethers (PBDEs), pose severe threats to global ecosystems and public health due to their environmental persistence, high potential for

bioaccumulation, and adverse toxicological effects. Marine ecosystems are major sinks for these contaminants, with POPs accumulating in sediments that subsequently pose as chronic secondary sources of pollution. Acknowledging this critical pressure, the European Green Deal, through the Marine Strategy Framework Directive, aims to protect marine environments and achieve "Good Environmental Status," whereby contaminant levels do not cause adverse effects [1]. Given the complexity of sediment-associated pollution, achieving this status requires a regional approach involving active site remediation. Remediation of severely contaminated zones is therefore a pressing regional priority in order to break the continuous cycle of secondary marine pollution.

As a prime example of such regional priorities, the Aliağa coastal zone in İzmir, Türkiye, particularly the area surrounding the shipbreaking yards, represents a critical marine environment that has been heavily affected by both historical and ongoing inputs of POP. Previous studies in this industrialized region have documented significantly elevated levels of PCBs, polycyclic aromatic hydrocarbons, and organochlorine pesticides in marine sediments [2–6] and in local aquatic biota, including commercial fish species [6]. Most recently, a comprehensive evaluation of the Aliağa coastline revealed that total PCB and PBDE concentrations in the surface sediments near shipbreaking facilities reached levels of up to 4750 ng/g and 5053 ng/g dry weight (dw), respectively [7]. This severe contamination profile, characterized by complex mixtures of aged pollutants, presents a realistic challenge that calls for engineered remediation strategies.

Bioremediation of PCB- and PBDE-contaminated sediments exploits the capacity of anaerobic microorganisms to reductively dehalogenate these compounds. During organohalide respiration, electrons from a donor such as H_2 are transferred through a respiratory complex to a reductive dehalogenase, which catalyzes the reduction in the halogenated substrate [8]. The availability of electron donors and cofactors depends closely on syntrophic interactions within the sediment microbial community. For example, non-dehalogenating community members can supply H_2 and corrinoids that support PCB-dechlorinating bacteria [9]. Electron supply can also be manipulated in engineered systems, including electro-assisted biodehalogenation [10]. These mechanisms provide a basis for examining how nutrient amendment and the addition of an enriched microbial culture affect reductive dehalogenation in contaminated sediments. Building upon these principles, previous studies investigated biostimulation and bioaugmentation strategies individually for PCB and PBDE-contaminated sediments [11–14]. For instance, bioaugmentation utilizing Dehalobium chlorocoercia DF1 successfully achieved a 56% reduction in highly chlorinated PCBs within 120 days in weathered sediments [11]. Similarly, biostimulation using formate and ethanol degraded fully brominated deca-BDE by 55% over the course of 180 days in laboratory-spiked lake sediments [15]. However, recent studies emphasized that simultaneous presence of mixed aromatic organohalides significantly altered degradation dynamics. For example, bioaugmentation using organohalide respiring bacteria (OHRB) was shown to approximately double the dehalogenation rates of PCBs and PBDEs in co-contaminated sediments compared to single-pollutant systems, which was attributed to the halopriming effect of contaminants [16]. Conversely, the presence of multiple PBDE congeners was found to decrease the degradation rates, which was attributed to competition for common dehalogenating bacteria [17]. Overall, the observed effects exhibit significant variations across different sediment systems. A key limitation of these studies was their use of freshly spiked sediments, which might not fully represent the complex dynamics in weathered sediments, where compound bioavailability could be limited. Therefore, a knowledge gap remains in the literature regarding the dehalogenation dynamics in chronically co-contaminated sediment profiles.

This study investigated the performance of bioremediation strategies for the anaerobic dehalogenation of PCBs and PBDEs in co-contaminated sediments. Microcosms were

established using environmentally aged sediments collected from the Aliağa shipbreaking yards to simulate three in-situ bioremediation strategies: bioaugmentation, biostimulation, and natural attenuation. These strategies were assessed to compare: (i) PCB and PBDE removal efficiencies and absolute dehalogenation rates, (ii) congener-level transformation pathways and the accumulation of lower-halogenated intermediates, (iii) shifts in the structure of the indigenous microbial community, and (iv) changes in the ecological risks associated with the treated sediments.

2. Materials and Methods

2.1. Chemicals and Reagents

This study targeted 46 PCB and 29 PBDE congeners (listed in Tables S1 and S2) using four standard mixtures: PCB-Mix 37 (18 PCB congeners; Dr. Ehrenstorfer GmbH, Augsburg, Germany), PCB Mix C-CS-01 (39 PCB congeners; AccuStandard, Inc., New Haven, CT, USA), BDE-COC (14 PBDE congeners; AccuStandard, Inc.), and BDE-OND (16 PBDE congeners; Wellington Laboratories Inc., Guelph, ON, Canada). Quality control standards included Mirex (internal standard), PCB-30 (2,4,6-CB), and PCB-185 (2,2′,3,4,5,5′,6-CB) from Dr. Ehrenstorfer GmbH, alongside BDE-77 (3,3′,4,4′-BDE) from AccuStandard, Inc. Single-congener standards of PCB-61 (2,3,4,5-CB) and BDE-47 (2,2′,4,4′-BDE) were procured from CPAchem Ltd. (Stara Zagora, Bulgaria) and AccuStandard, Inc., respectively. All the solvents used for the pretreatment of samples (i.e., hexane, and acetone) were of gas chromatography grade. Solvents, alumina, copper powder, and anhydrous sodium sulfate were Supelco solutions obtained from Merck KGaA, Darmstadt, Germany.

2.2. Study Area and Sample Collection

Sediment samples were collected from the coastal zone of shipbreaking yards in Aliağa, located approximately 45 km north of İzmir, Türkiye, in May 2023. This area has been subject to intensive ship-dismantling operations since 1977. As a result of these activities, the sediments were contaminated with POPs [7]. Surface sediments (0–10 cm) were collected using a Hydro-Bios Van Veen grab sampler from three points within a 0.3 km^2 area. The collected samples were immediately transferred into hexane-washed glass jars, sealed to prevent contamination, and stored in the dark. Upon transportation to the laboratory, the samples were kept at 4 °C until further analysis.

2.3. Enrichment of Anaerobic Bacterial Cultures

An inoculum was derived from the native sediment, ensuring that the enriched halorespiring consortium was highly adapted to the local, extensively weathered co-contamination profile. For the enrichment, a composite sediment sample was prepared by passing the wet samples through a 2-mm industrial sieve to preserve native microbial viability. Initially, one gram of wet composite sediment was inoculated into 100 mL of artificial seawater-based medium (ASM) prepared in 250 mL serum bottles under an N_2:CO_2:H_2 (78%:20%:2%) atmosphere in the anaerobic chamber. The ASM growth medium was based on artificial seawater (AS), prepared as described by Berges et al. [18], and supplemented with a mineral and vitamin solution [19]. The components of AS and ASM are presented in Table S3. Resazurin was added as a redox indicator, and yeast extract was included to supply additional essential nutrients. Sodium acetate (10 mM) was the non-halogenated carbon source, and the H_2 in the initial bottle headspace was available as a potential electron donor, while PCB-61 (140 ppb) and BDE-47 (15 ppb) were added as electron acceptors at concentrations ten times their water solubility. Additional H_2 was not supplied directly to the sealed culture bottles during incubation, and its concentration was not monitored. Following an initial incubation, three sequential subcultures were

established by transferring 10% (*v*/*v*) of the inoculum into fresh ASM, with contaminant concentrations progressively increasing at each transfer (by factors of 1.0, 1.2, 1.4, and 1.6, respectively) to promote microbial adaptation toward an organohalide-transforming population. During transfers into fresh medium, the anaerobic chamber was continuously flushed with the gas mixture to maintain anoxic conditions. Inside the chamber, liquid samples were routinely withdrawn via syringe through the septa to monitor depletion of PCB-61 and BDE-47 using the method described by Demirtepe and Imamoglu [15]. Subculturing into fresh medium was performed once the spiked electron acceptor concentrations declined by >40%. All enrichments were conducted in duplicate and incubated at 25 °C without agitation.

2.4. Sediment Microcosms

Homogenized composite sediment was kept in the anaerobic chamber for three days before preparation of the microcosms. Its total organic carbon, analyzed using Shimadzu TOC-Vcph (TNM-1/SSM-5000A, Kyoto, Japan), Analytik Jena Multi N/C 3100 analyzer (Jena, Germany), was 4.58% ± 0.77%. For each microcosm set, 86 g of wet composite sediment was combined with 100 mL of the corresponding liquid layer in 250 mL serum bottles. In the bioaugmentation (BA) microcosms, composite sediment was amended with the enriched microbial culture. For the biostimulation (BS) set, the ASM growth medium, autoclaved to prevent any microbial addition, was added to the sediments. This set aimed to boost the activity of indigenous microorganisms; it contained all the micronutrients present in the ASM, including the yeast extract and sodium acetate. In the natural attenuation (NA) set, only filtered (0.22 μm) AS, without any micronutrients, was used. A negative control (NC) set was established to distinguish the effects of added spent growth medium from those of microorganisms in the BA set. Hence, the liquid layer was a filtered (0.22 μm) enriched microbial culture. The sterile control (SC) microcosms contained composite sediment and filtered AS, along with 0.5 mg of mercuric chloride per gram of sediment to inhibit microbial activity. To ensure sterile conditions throughout long-term operation, SC microcosms were autoclaved for three consecutive days at 120 °C under 1.1 atm pressure for 20 min each time. The summary of the microcosm sets is presented in Table 1. The BA, BS, and NA microcosms were prepared in triplicate, and the NC and SC microcosms were prepared in duplicate. All the microcosms were prepared in an anaerobic chamber under N_2:CO_2:H_2 (78%:20%:2%) atmosphere, sealed with butyl-rubber septa, and incubated at 22 °C in the dark for 198 days. Sediment samples were collected at four-week intervals by opening the bottles inside the chamber, where the atmosphere was flushed with N_2:CO_2:H_2 (78%:20%:2%) to control oxygen levels during sampling. After sample collection, the bottles were resealed with septa and crimp caps before removal from the chamber. No H_2 was injected directly into the bottles, and H_2 concentrations within the bottles were not measured during incubation.

Table 1. Microcosm set ingredients (ASM: artificial seawater medium; AS: artificial seawater).

Microcosm Type	Set Name	Composite Sediment	Liquid Medium
Bioremediation Sets	Bioaugmentation	+	Enriched culture in ASM
	Biostimulation	+	C source and nutrient-rich ASM (autoclaved)
	Natural Attenuation	+	Filtered AS
Control Sets	Negative Control	+	Filtered enriched culture in ASM
	Sterile Control	+ (autoclaved)	Filtered AS

+ sediment is added in the set.

2.5. Extraction and Analysis of PCBs and PBDEs

At four-week intervals, ~2 g wet sediments were collected from each microcosm bottle. Sediment samples were kept at −20 °C overnight and freeze-dried for 48 h. Approximately one gram of dry sample was mixed with 2 g of anhydrous sodium sulfate and spiked with PCB-30, PCB-185, and BDE-77 as surrogate standards. After an overnight soak in a 30 mL hexane:acetone mixture (1:1 *v*/*v*), samples were extracted twice in an ultrasonic bath for 30 min each, using a fresh solvent mixture in the second run. Copper powder was added to the extraction solvents to remove sulfur. The two extracts were combined and concentrated to 2–5 mL by rotary evaporation. To remove interfering organic compounds, the colored extract was treated with concentrated sulfuric acid (1:1.5 *v*/*v*) according to US EPA Method 3665A [20]. The clear top layer of the extract was purified by passing it through a column containing 0.5 g of 6% deactivated alumina, topped with anhydrous sodium sulfate, and eluting with 2 mL of hexane. Finally, the purified extract was concentrated to 1 mL under a high-purity nitrogen stream.

Water phase samples (1 mL) were collected from each microcosm bottle at the end of incubation. Samples were mixed with 5 mL of hexane, hand-shaken for 10 s, then vortexed for 1 min. After centrifugation, the hexane layer was carefully syringed and passed through a Pasteur pipette column packed with 0.5 g alumina and 0.04 g Cu powder, topped with anhydrous sodium sulfate. Additionally, 1 mL of hexane was eluted after the sample, and all eluate was collected and concentrated to 1 mL under a high-purity nitrogen stream.

The extracts were spiked with Mirex as the internal standard (50 ppb) and analyzed using an Agilent 8890N gas chromatograph coupled to a 5977C mass spectrometer (GC-MS, Waldbronn, Germany). For PCB analysis, the target compounds were measured in electron impact ionization (EI) mode using an Agilent DB-5MS capillary column (30 m × 0.25 mm × 0.25 μm, CA, USA). The oven program started at 60 °C, was held for 1 min, then increased to 170 °C at a rate of 20 °C/min (3 min), later continued to increase to 200 °C at 3 °C/min (2 min), and to 300 °C at 8 °C/min (3 min). The injection volume was 1 μL in pulsed splitless mode, and the temperatures of the MSD transfer line, ion source, and inlet were 280 °C, 230 °C, and 250 °C, respectively. The carrier gas was helium at a flow rate of 1.1 mL/min. The target PCBs were analyzed in selected ion monitoring (SIM) mode using the quantifier and qualifier ions given in Table S1.

For PBDE analysis, the target compounds were measured in EI mode using an Agilent DB-5MS capillary column (15 m × 0.25 mm × 0.10 μm). The oven program started at 150 °C, was held for 2 min, then increased to 250 °C at 15 °C/min (2 min), and finally to 325 °C at 20 °C/min (8 min). The injection volume was 2 μL in pulsed splitless mode, and the temperatures of the MSD transfer line, ion source, and inlet were 280 °C, 300 °C, and 250 °C, respectively. The carrier gas was helium at a flow rate of 1.2 mL/minute. The target PBDEs were analyzed in SIM mode using the quantifier and qualifier ions given in Table S2.

2.6. QA/QC

Individual congeners were identified by matching retention times and quantifier/qualifier ion ratios against certified reference standards. Under the applied chromatographic conditions on the DB-5MS capillary column, all target congeners were baseline-resolved except for two co-eluting PCB pairs (PCB-66/95 and PCB-151/82) and one co-eluting PBDE group (BDE-198/199/200/203), which were quantified as combined peaks (Tables S1 and S2). To validate the sample pretreatment protocol, laboratory control sediment samples were analyzed in our laboratory, and the results were reported in our previous study. We obtained satisfactory analyte and surrogate recoveries (65–116% for PCBs, and 99–121% for PBDEs [7]). Water laboratory control samples showed acceptable

recoveries for the analytes and surrogate standards (61–94% for PCBs, and 68–106% for PBDEs). Surrogate standard recoveries were checked for every sediment sample (n = 104). Recoveries for PCB-30, PCB-185, and BDE-77 were 118.9 ± 25.7%, 105.8 ± 25.8%, and 74.1 ± 15.9%, respectively. Recovery correction was not applied to the samples. Blanks were analyzed in every batch of 13 samples (n = 8), and surrogate recoveries in blank samples were 81.5 ± 11.5%, 79.6 ± 23.6%, and 107.1 ± 7.92% for PCB-30, PCB-185, and BDE-77, respectively. Blank correction was not performed for sediment samples, while analyte concentrations in blanks were subtracted from those in water samples. The calibration ranges for PCBs were 1–400 ppb (2–800 ppb for PCB-28, -52, -99, -110, -146, -153, -138, -187, -177, and -180), while those for PBDEs were 1–50 ppb (BDE-17 to -190), 1.2–36 ppb (BDE-198 to -205), 3–90 ppb (BDE-206, -207, and -208), and 8–340 ppb (BDE-209). The calibration curves for all congeners had $R^2 > 0.99$. The method detection limits (MDL) were identified either by analyzing the lowest calibration standard 10 consecutive times or by computing the average plus three standard deviations of the analytes in blank samples. The limits of quantitation (LOQ) were then computed as 3.18 times the MDL values. Detection limits for individual compounds are presented in Supplementary Materials Tables S1 and S2. The congeners detected below the LOQ (BDL), considering all microcosm samples, were BDE-202 (Detection frequency (DF) = 0%), PCB-147 (DF = 0%), BDE-198/199/200/203 (DF = 2%), BDE-190 (DF = 3%), BDE-201 (DF = 5%), and PCB-173 (DF = 8%), and were excluded from further calculations. For five congeners, with 25% < DF < 99%, BDL values were replaced with LOQ/2.

2.7. DNA Extraction and Shotgun Metagenomic Sequencing

To characterize microbial community shifts during incubation, total genomic DNA was extracted from the initial composite sediment (Day 0) and from the BA, BS, and NA microcosms collected at the end of the incubation using the GeneMATRIX Soil DNA Purification Kit (EURx Sp. z o.o., Gdańsk, Poland). Metagenomic sequencing was performed to compare microbial responses across the three bioremediation strategies. Library preparation and metagenomic sequencing were performed using the Illumina platform with a paired-end sequencing strategy. The quality of the raw sequencing reads was evaluated using FastQC. Subsequently, low-quality reads and adapter sequences were removed using Trimmomatic. Taxonomic classification of the metagenomic data was performed using Kraken2 software (version 2.1.3) against the RefSeq reference database. Alpha-diversity metrics, including Shannon (H′) and Simpson (1-D) indices, were calculated to assess community richness and evenness.

2.8. Data Analysis

The dehalogenation rates were computed as the reduction in the total number of halogen atoms per molecule over time. This rate is typically expressed as the difference between the initial and final-day total halogen numbers per biphenyl or diphenyl ether divided by the 198-day incubation period (Cl/bp/d and Br/dp/d) [11,15,16,21]. The degradation kinetics of BDE-209 were explained by the pseudo-first-order model, with a rate constant k (d^{-1}).

Net contaminant removal efficiencies were calculated based on total mass concentrations (ng/g dry weight) in the sediment phase relative to initial concentrations $\left(1 - \left(\frac{C}{C_0}\right) \times 100\right)$.

Our study objectives included evaluating changes in the ecological risks associated with POPs in sediments. To achieve this, risk quotients (RQ) were estimated using Equations 1 and 2 [22]. Chronic and sublethal RQs were computed using the concentration of target compounds in the sediment (C_m) and the predicted no-effect concentration in the

sediment ($PNEC_{sed}$), which was estimated by the no observed effect concentration (NOEC) or lethal concentration 50% (LC50) obtained from the US EPA's ECOTOX database (mg/L) [23], sediment organic carbon–water distribution coefficients (K_{oc}) of the congeners (from EPISUITE), and the sediment organic-carbon fraction (f_{OC}). Since the ECOTOX database presents endpoints derived from various studies, the median of the values was used (Table S4). Assessment factors (AF) were set to 100 and 1000 for the NOEC and LC50 endpoints, respectively. As a result, risk levels were categorized as minimal (RQ < 0.01), low (0.01 ≤ RQ < 0.1), moderate (0.1 ≤ RQ < 1), and high (RQ ≥ 1) [24].

$$RQ = \frac{C_m}{PNEC_{sed}} \quad (1)$$

$$PNEC_{sed} = \frac{(NOEC\ or\ LC50) \times K_{oc} \times f_{oc}}{AF} \quad (2)$$

The statistical analysis was performed using IBM SPSS 25. Analysis of variance (ANOVA) was used to identify variance within the data set for a reactor and to compare reactors; results were considered significant at $p < 0.05$.

3. Results and Discussion

3.1. Dehalogenation Efficiency and Rates During Bioremediation

Total PCB and PBDE concentrations were tracked over 198 days to quantify net mass removal under BA, BS, NA, NC, and SC conditions. The removal efficiency is expressed as the sediment mass concentration at any time relative to the initial concentration (C/C_0) for each microcosm set in Figure 1A,B. For both POPs, SC exhibited only minor fluctuations attributable to analytical variability, while overall concentrations remained essentially constant (two-way ANOVA without replication, $p > 0.05$). This indicated that abiotic losses were negligible under the experimental conditions.

By day 198, net sediment-mass decreases in ΣPCB mass reached 44% in BS, 42% in BA, 27% in NC, and 11% in NA (Figure 1A). Final concentrations in all sets were significantly different from those in the SC set ($p < 0.05$). Importantly, the higher net removal in NC than NA highlighted the role of liquid medium composition (Tables 1 and S3). While NA received only inorganic artificial seawater (AS) devoid of exogenous carbon or nutrients, the higher removal in NC suggested that residual constituents carried by the filtered spent medium (e.g., remaining C source, macronutrients, trace metals, vitamin B12, soluble microbial metabolites/exudates produced during enrichment, and partially degraded PCB-61 and BDE-47 with their possible products) were sufficient to stimulate indigenous activity beyond the unamended condition, while enriched consortia addition achieved a higher mass removal in BA. Net decreases in ΣPBDE mass were 48% in BS, 35% in BA, 28% in NC, and 10% in NA over 198 days (Figure 1B), with the SC set having significantly different final concentrations from the other reactors ($p < 0.05$). Although BS and BA efficiencies were similar for ΣPCB mass reduction, BS was more efficient at removing ΣPBDE mass. Similar to ΣPCBs, amended treatments substantially outperformed NA. These results indicated an obvious benefit from active amendment strategies. This observation was similar to a study, in which periodic short-chain fatty acid amendments provided an additional 7.6–10.3% reduction in total PCBs relative to non-amended controls [25]. It should be noted that while statistical stability of the sterile control ruled out abiotic losses, the net sediment mass reductions reported above reflected overall contaminant depletion from sediments, involving molecular weight loss from halogen removal, transformation into unquantified end-products, and partial water-phase partitioning of lower-halogenated congeners (detailed in Section 3.2). Therefore, actual reductive dehalogenation

activity was specifically distinguished and quantified by reductions in the total number of halogen atoms per molecule, as discussed below.

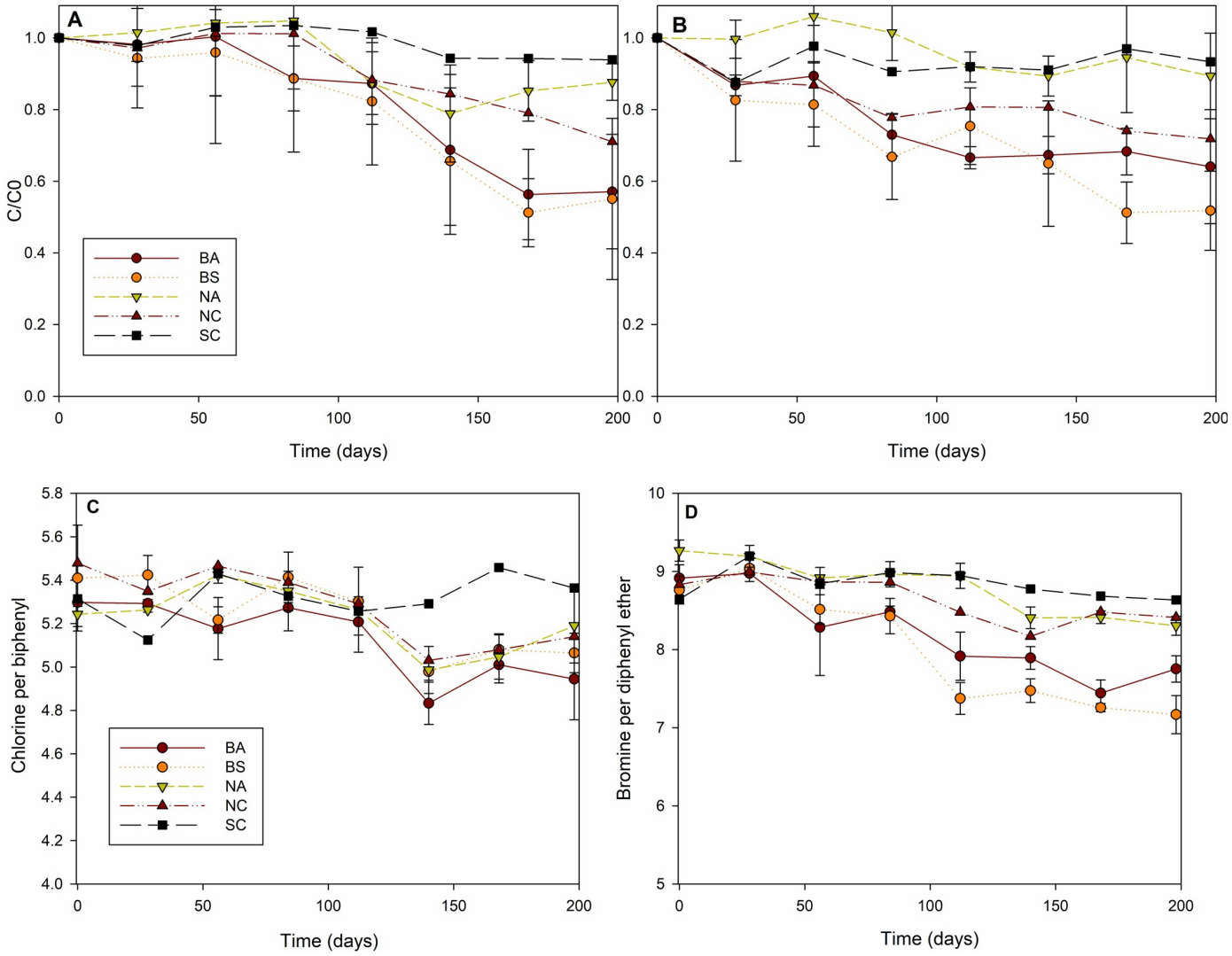


Figure 1. (**A**) The ratio of total PCB and (**B**) PBDE concentration at each time to the initial concentration for microcosm sets. (**C**) Chlorine per biphenyl and (**D**) bromine per diphenyl ether change with time in microcosms. Values represent the average across triplicate reactors for the bioaugmentation (BA), biostimulation (BS), and natural attenuation (NA) sets, and duplicate reactors for the negative control (NC) and sterile control (SC) sets. Error bars show the standard deviations of triplicate reactors.

The presence of co-contaminants resulted in preferential dehalogenation across the microcosm sets. The BA set exhibited a lag period in PCB reduction during the first 56 days, while PBDEs were actively degraded over the same period. Conversely, as PCB removal accelerated between days 56 and 168, PBDE reduction slowed and plateaued after day 112. The BS set showed a similar trend, except that PBDE removal continued until day 168 with minor slowdowns. Regarding PCBs, the NA and NC sets remained relatively stable through day 84. For both contaminants, NA showed minimal reduction between days 84 and 112, stabilizing thereafter. While amendments in NC stimulated initial PBDE removal, degradation slowed after day 84, when PCB removal started. Overall, our microcosm studies indicated that weathered co-contaminants may serve as preferred electron acceptors for indigenous microbes when stimulated by micronutrients or enriched consortia. Furthermore, the initial lag phase observed for PCBs across all sets can be

attributed to the greater ease of carbon-bromine bond cleavage during reductive dehalogenation relative to carbon-chlorine bonds [26]. Additionally, differences in molecular structure, thermodynamic favorability, and enzyme specificity may play a crucial role in selective dehalogenation. Specifically, the flexible ether linkage and higher redox potentials of PBDEs make them thermodynamically more favorable electron acceptors [27,28], while reductive dehalogenases (RDases) within the native consortium may exhibit higher substrate affinity or faster induction kinetics toward brominated aromatic substrates [16,17].

Our findings were contrary to the results of previous studies. In sediments bioaugmented with *Dehalococcoides* strains, the dehalogenation of co-contaminants, PCBs, PBDEs, and tetrabromobisphenol A, was initiated simultaneously [16]. Tetrachlorooethene and penta-BDE underwent synchronous dehalogenation without any apparent organohalide substrate selectivity by the bacteria [29]. This variability might be caused by the weathered sediments and enriched microbial consortia used in our study. In historically contaminated sediments, POPs become deeply embedded and bound within the organic fraction of the sediment matrix, restricting their initial bioavailability. Specific PBDEs may exhibit slightly higher bioavailability [30], and lower dehalogenation activation energies than PCBs, as mentioned previously. Additionally, OHRB, such as *Dehalococcoides*, might require a higher cell density threshold to initiate dehalogenation of specific contaminants, such as PCBs [16]. Taken together, probably lower cell density in our sediments could initiate more bioavailable PBDE dehalogenation, leading to a priming effect for further PCB degradation.

Dehalogenation was also monitored by tracking the change in the total number of halogens per molecule over time (Cl/bp and Br/dp). Figure 1C,D present the Cl/bp and Br/dp changes over time, respectively. The trends observed in the figure supported the discussion on preferential electron acceptors for indigenous species. For PCBs, the dehalogenation rates (Cl/bp/day) over 198 days followed the order BA (0.00178) > BS (0.00174) > NC (0.00171) > NA (0.000269). The rate in BA slightly exceeded BS, indicating the long-term efficacy of the enriched anaerobic culture in reducing the chlorine load. When evaluating the overall dehalogenation rates of PBDEs, BS emerged as the most efficient strategy (0.00805 Br/dp/day) and outperformed BA (0.00587) > NA (0.00486) > NC (0.00213). The NC set performed better in PCB dehalogenation, yet its rate remained far below that of other treatments for PBDEs. The rates were compared across microcosms using one-way ANOVA followed by Tukey's post-hoc test ($\alpha = 0.05$). For PBDEs, the dehalogenation rate in BS was significantly higher than in NC ($p < 0.05$), demonstrating the stimulatory effect of nutrient and carbon amendment, whereas no statistically significant difference was observed between BA and BS ($p > 0.05$), indicating comparable dehalogenation kinetics with or without culture addition. In contrast, PCB dehalogenation rates did not differ significantly among the treatments ($p > 0.05$), likely reflecting the longer lag phase observed in all microcosms, lower overall extent of dehalogenation, and inter-replicate variability.

Our findings fell within the ranges reported in the literature, although sediment history and applied bioremediation strategies significantly shaped these kinetics. For instance, in highly contaminated field sediments from Lake Hartwell, natural attenuation rates were reported at 0.000258 Cl/bp/day [31], whereas bioaugmentation in Baltimore Harbor sediments reached 0.0041 Cl/bp/day [11]. Similarly, in laboratory-spiked Baltimore Harbor sediments, dehalogenation rates were reported as 0.0043 Cl/bp/day for biostimulation with electron donors [32], 0.0036 Cl/bp/day for biostimulation with fatty acids [33], and 0.0059 Cl/bp/day for bioaugmentation using a four-strain microbial consortium [34]. Our PBDE dehalogenation rates were higher than those reported by Demirtepe and Imamoglu (2019), who observed rates of 0.0012, 0.0011, and 0.0009 Br/dp/day for BS,

BA, and NA, respectively, in deca-BDE-spiked sediments [15]. Bioaugmentation with specific *Dehalococcoides* strains in penta-BDE spiked sediments achieved much higher rates, up to 0.0715 Br/dp/day [29]. The rates achieved in the present study emphasized the substantial potential of the indigenous microbial environment. The targeted addition of micronutrients and carbon sources to the BS treatment effectively stimulated native OHRB populations, even within a complex, co-contaminated sediment matrix. Specifically, regarding electron donor dynamics, although all microcosms shared the same initial H_2-containing headspace (2%) and identical 4-week sampling inside the anaerobic chamber, the markedly lower activity in NA compared with BS indicated that passive headspace H_2 alone was insufficient to sustain high dehalogenation rates. While obligate OHRB such as *Dehalococcoides* require H_2 as the direct electron donor and utilize acetate as a carbon source[35], in mixed sediment communities, amended acetate and yeast extract also indirectly support dehalogenation by stimulating fermentative and syntrophic microbes that supply slow, sustained fluxes of H_2 [36–38].

Unlike the complex interconversion of intermediate congeners, the fully brominated deca-BDE (BDE-209) serves exclusively as a parent compound, allowing its degradation to be modeled using first-order reaction kinetics ($\ln C = \ln C_0 - kt$). The calculated first-order degradation rate constants (k) for BDE-209 revealed that BS achieved the highest k (0.0046 day^{-1}, $R^2 = 0.97$), followed by BA (0.0034 day^{-1}, $R^2 = 0.91$) and NA (0.0016 day^{-1}, $R^2 = 0.87$). These values agree with the literature. For instance, Demirtepe and Imamoglu (2019) reported highly comparable k's for laboratory-spiked lake sediments under BS (0.0049 day^{-1}), BA (0.0028 day^{-1}), and NA (0.0025 day^{-1}) [15]. Across various studies, k values for BDE-209 range from 0.00013 day^{-1} [39] to 0.041 day^{-1} [40] in laboratory-spiked sediments. This was particularly notable given the historically weathered nature of the Aliağa sediments, as freshly spiked sediments typically exhibit faster degradation kinetics.

3.2. Homolog Dynamics During Bioremediation

Homolog-group analysis (nmol/g dry weight) revealed treatment-specific redistribution of PCBs and PBDEs consistent with anaerobic reductive dehalogenation (Figure 2). In this analysis, PCB and PBDE homolog groups represent the summed concentrations of the targeted congeners sharing the same degree of halogenation, spanning mono- through nona-CBs (46 congeners) and tri- through deca-BDEs (29 congeners), respectively, with the exact congener composition of each homolog group detailed in Tables S1 and S2. The BA strategy resulted in the depletion of highly chlorinated CBs, yielding net decreases of 53.2% in hexa-CBs, 43.0% in hepta-CBs, and 59.8% in octa-CBs by day 198, whereas the quantified nona-CB homolog, PCB-206, decreased only by 20.6% (Figure 2A). In our study, lower-chlorinated PCBs exhibited transient increases and decreases, indicating intermediate formation followed by consumption as dehalogenation progressed. At the end of incubation, the end-product of dehalogenation, mono-CBs, increased by 52%. However, this increase did not stoichiometrically correspond to the decrease in higher-chlorinated congeners. This discrepancy was primarily attributed to our inability to measure all potential intermediate species generated during the transformation pathways. Additionally, decreasing trends observed in di and tri-CBs suggested possible partitioning into sediment porewater, followed by migration to the overlying water layer. To test this hypothesis, we sampled overlying water at day 198, and established a combined sediment-water molar mass balance (Table S5). While sediment-only molar mass balance in BA declined to 58% by day 168, incorporating water-phase PCB mass at day 198 increased the mass balance to 86%. In the overlying water, lower chlorinated congeners such as PCB-9 (10.8%), PCB-6 (6.98%), PCB-4 (6.41%), PCB-1 (6.37%), PCB-8 (6.07%), and PCB-52 (5.69%) were found at higher mole percentages than parent congeners (Figure S1A). Together with

the observed decrease in Cl/bp ratios, these results confirmed that reductive dehalogenation formed less hydrophobic daughter products that subsequently partitioned from the sediment into the water phase. Overall, BA using a site-specific enriched consortium led to the degradation of higher PCBs without the need for external non-native inoculants.

Biostimulation demonstrated a clear two-phase homolog-group response, characterized by a steady decrease in highly chlorinated PCBs until day 112, followed by a steep decrease on day 140 (Figure 2B). Unlike BA, nona-CB showed a steady, clear decrease, reaching a 53.1% reduction on day 198. However, PCB-206 showed a minor rebound in the final interval. Although reductive dehalogenation of unquantified decachlorobiphenyl (PCB-209) could theoretically contribute to the nona-CB formation, this possibility remained purely speculative without direct PCB-209 measurement and the minor late-stage fluctuation may alternatively reflect analytical variability or micro-scale sediment heterogeneity. Over the incubation period, net decreases were 62.6% in octa-CBs, 38.5% in hepta-CBs, 50.2% in hexa-CBs. In lower-CBs, although sudden increases were observed, concentrations decreased relative to initial-day concentrations. An increase by 24.1% in mono-CBs did not correspond to these decreases. Overlying water analysis revealed higher percentages of PCB-9 (11.6%) and PCB-52 (5.25%), but not mono-CBs (Figure S1B). Hence, the decreases observed in mono-CBs at various time points were attributed either to analytical errors or to congeners remaining in the sediment pore-water. Consistent with this partitioning behavior, while the sediment-phase PCB molar mass balance in the BS microcosms declined to 53% by day 168, incorporating the water-phase PCB mass on day 198 increased the combined molar recovery to 73% (Table S4). The remaining molar deficit in BS likely reflects the formation of unquantified biphenyl. Overall, steady decreases in higher-CBs under BS reflected the successful activation of indigenous microbial populations through targeted nutrient and electron-donor amendments. While alternative strategies, such as the halo-priming approach by Xu et al. (2019) [41], stimulated the reduction in highly chlorinated Aroclor 1260 homologs (hexa- through nona-CBs by 6.5% to 28.3%) over 120 days, our findings demonstrated that such halogenated primers were not strictly necessary. The BS strategy employed in this study, i.e., relying solely on non-halogenated carbon sources (acetate) and essential micronutrients/vitamins, yielded substantial degradation of highly chlorinated homologs. This highlighted the remarkable intrinsic dehalogenation capacity of the weathered sediment microbiome when provided with appropriate nutritional support.

Under NA, homolog-level changes were limited and more variable. Hexa-CBs decreased by 31.4% and octa-CBs by 17%, whereas hepta-CB showed a slight increase by 3.2% at the end of 198 days. Throughout incubation, the formation of hexa-, hepta-, and octa-CBs was more prominent compared to BA and BS sets, where decreasing patterns almost always dominated. This indicated a slow dehalogenation of higher-CB under NA. Lower-chlorinated homologs changed marginally. This pattern also suggested slow intrinsic transformation without amendment-driven strategy. Another important observation was for the overlying water samples. The PCB profile in the water samples differed markedly from that of BA and BS; PCB-18 (7.65%), PCB-28 (7.15%), PCB-22 (6.13%), and PCB-66/95 (5.26%) were more dominant in NA.

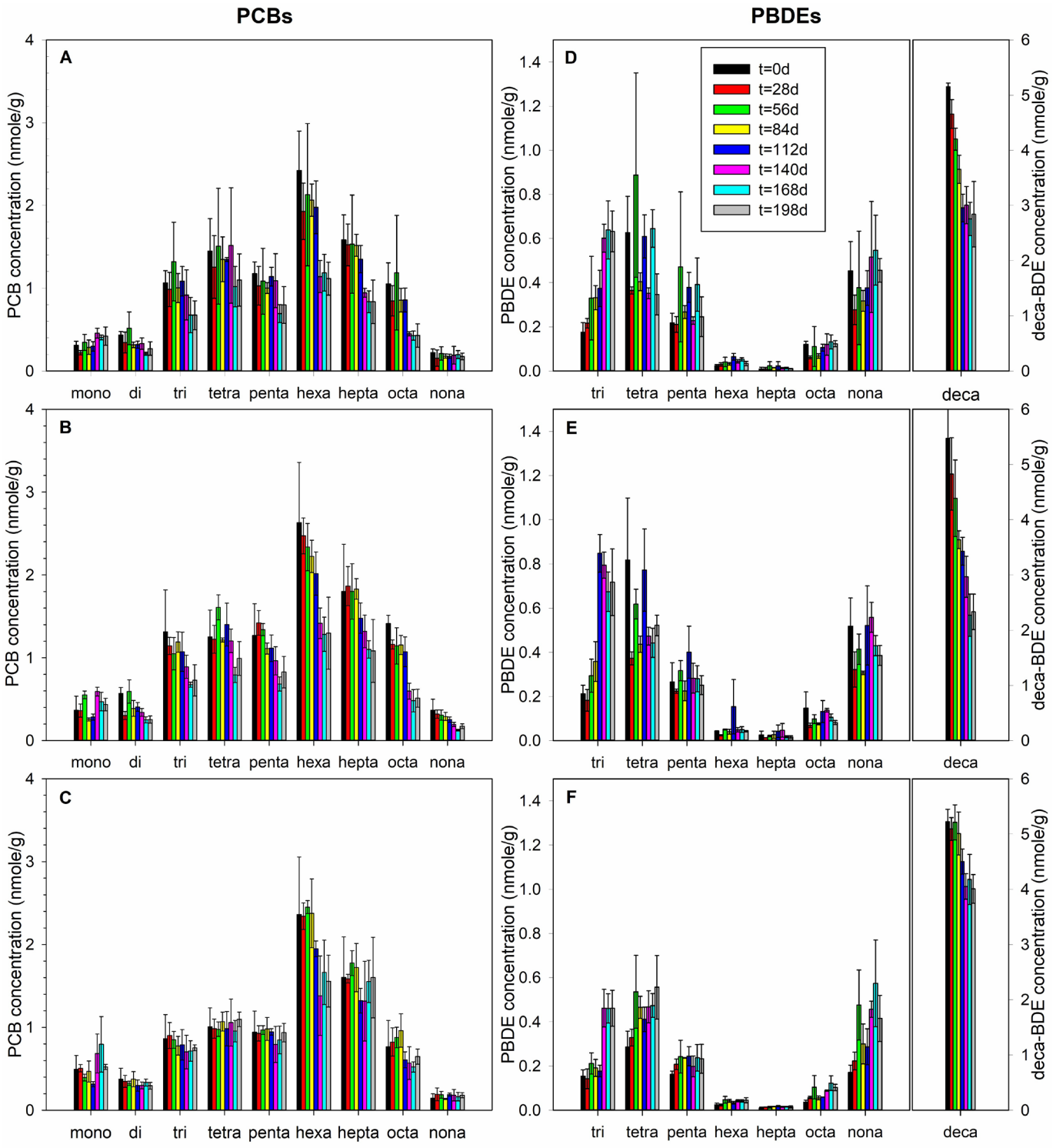


Figure 2. PCB and PBDE concentrations of quantified homolog groups in bioaugmentation (**A**,**D**), biostimulation (**B**,**E**) and natural attenuation (**C**,**F**) microcosms with respect to time. Deca-BDE concentrations are given in the right-hand side *y*-axis. Each homolog bar represents the sum of all quantified target congeners with the corresponding number of chlorine or bromine substituents, as listed in Tables S1 and S2.

The degradation of PBDEs in the microcosms exhibited a clear sequential dehalogenation pattern, characterized by the depletion of highly brominated congeners, notably the deca-BDE BDE-209, and the concurrent accumulation of lower brominated intermediates. In the BA microcosms, deca-BDE decreased by 45% by day 198 (Figure 2D). This depletion led to the progressive accumulation of lower brominated intermediates. Tetra- through nona-BDEs exhibited fluctuating patterns of decrease and accumulation, whereas tri-BDEs accumulated continuously, marking a 260% increase by the end of the incubation.

The BS treatment demonstrated the most robust dehalogenation performance for PBDEs. Deca-BDE concentrations decreased continuously until day 168, achieving a 56% net reduction (Figure 2E). This was accompanied by a transient accumulation of tetra- through nona-BDEs. The terminal quantified homolog, tri-BDEs, increased by 300% up to day 112 and ended with a 238% net increase, indicating further transformation into further downstream products. The lack of analytical standards for di- and mono-BDEs limited the complete tracking of downstream dehalogenation products. Additionally, water-phase concentrations were BDL across all microcosms at day 198, indicating that partitioning into the overlying water was negligible due to their higher hydrophobicity. Therefore, an exact stoichiometric closure between BDE-209 depletion (i.e., −3.14 nmole/g dw) and quantified daughter congeners' formation (i.e., +0.28 nmole/g dw) cannot be established. Consequently, the incomplete molar mass balances observed in the sediment phase by day 198 for BA (69%) and BS (58%), in contrast to the near-complete mass balance in the sterile control (93%, Table S6), can be attributed to genuine reductive dehalogenation into unquantified lower-brominated or non-brominated end-products (e.g., di-/mono-BDEs and diphenyl ether), alongside potential formation of non-extractable bound residues and analytical uncertainties [15,42,43].

Contrary to BA and BS microcosms, NA exhibited a delayed and restricted dehalogenation profile (Figure 2F). Deca-BDE levels decreased slightly for the initial 84 days, ultimately yielding only a 33% reduction by day 198. This limited primary degradation resulted in a massive "bottleneck" accumulation of highly brominated intermediates, with hepta-, octa-, and nona-BDEs increasing by 184%, 185%, and 142%, respectively. This pronounced lag phase and the accumulation of high-bromine intermediates confirmed that while an intrinsic dehalogenation potential existed in these historically contaminated sediments, the rate was limited without active intervention. Because the NA microcosms contained only inorganic AS without added carbon or nutrients (Table S3), this intrinsic dehalogenation was likely sustained by endogenous fermentable substrates as well as sediment-associated redox-active organic matter. Specifically, insoluble humic fractions such as humin within the organic-rich Aliağa sediment (TOC: 4.58 ± 0.77%) can act as extracellular electron donors or redox mediators to support microbial dehalogenation under oligotrophic conditions [44,45].

3.3. Dehalogenation Pathways

Based on the individual congeners resolved via retention time matching and quantifier/qualifier ion ratios (Tables S1 and S2), mole percentage shifts from initial to final days of operation (Figure S2) and time-resolved molar concentrations (nmol/g dw; Figures S3–S6) were evaluated to propose dehalogenation pathways. For PCBs, the most abundant congeners at t = 0, i.e., PCB-138 (2,2′,3,4,4′,5′-CB) and PCB-153 (2,2′,4,4′,5,5′), were suggested to be transformed to PCB-99 (2,2′,4,4′,5) by meta-Cl removal, and to PCB-87 (2,2′,3,4,5′) and PCB-101 (2,2′,4,5,5′) by para-Cl removal, respectively, in both BA and BS strategies. PCB-101 might further be dehalogenated to form PCB-52 (2,2′,5,5′) and then PCB-18 (2,2′,5), since their mole% increased strikingly. The proposed pathways were observed in previous studies [25,46]. An interesting observation was that mole% of PCB-180 (2,2′,3,4,4′,5,5′), the parent of PCBs-138 and -153, increased in BS, while it slightly

decreased in BA. The possible parent of PCB-180 could be PCB-194, which substantially decreased by 2.6% in BS. Consistent with sequential dehalogenation, temporal profiles in both BA and BS showed continuous depletion of parent hepta- and hexa-CBs (e.g., PCB-180, PCB-138, and PCB-153), accompanied by transient accumulation of intermediate penta- and tetra-CBs, most notably PCB-52 peaking at day 56 in BS and days 56–140 in BA, followed by their subsequent decline as tri-chlorinated PCB-18 accumulated (Figures S3 and S4). Because lower-chlorinated intermediates partially partitioned into the water phase (Section 3.2) and unquantified lower-CBs or biphenyl were outside the targeted SIM analyte list, daughter congener accumulation in the sediment did not stoichiometrically match total parent depletion.

The ultimate parent congener, BDE-209 (2,2′,3,3′,4,4′,5,5′,6,6′-BDE), dehalogenated to form BDE-206 (2,2′,3,3′,4,4′,5,5′6-BDE), BDE-207 (2,2′,3,3′,4,4′,5,6,6′-BDE), and BDE-208 (2,2′,3,3′,4,5,5′6,6′-BDE) by ortho-, meta-, and para-Br removal, respectively. Further dehalogenation of these intermediates resulted in greater accumulation of BDE-207 and -208 in BA, and BDE-206 in BS at the end of incubation (Figures S2B, S5 and S6). Temporal PBDE profiles also demonstrated that nona-BDEs exhibited transient intermediate increases between days 112 and 168 before declining toward day 198. Previous studies identified varying dominant products of BDE-209, possibly due to sediment characteristics and treatment strategies applied [47,48]. Possible dehalogenation of penta-BDEs, i.e., BDE-99 (2,2′,4,4′,5) and BDE-100 (2,2′,4,4′,6), formed BDE-47 (2,2′,4,4′) and BDE-66(2,4,3′,4′). However, BDE-47 dehalogenation rate was much higher than its formation, so its mole% decreased, with a more pronounced decline in BA. Among the tri-BDEs, BDE-28 (2,4,4′) formation was more dominant than BDE-17 (2,2′,4) in both strategies. Selective formation of tri-BDEs was also noted in varying environmental conditions [13,15,17,27]. Overall depletion of BDE-47 coincided with sustained accumulation of the tri-brominated products BDE-28 and BDE-17. Notably, the molar increase in BDE-28 and BDE-17 accounted for only part of the net molar loss of BDE-47 and higher-brominated congeners (Figures S5 and S6), reflecting further sequential debromination into terminal di- and mono-brominated diphenyl ethers (di-BDEs and mono-BDEs) that were not included in the target SIM calibration suite (Table S2). Overall, it can be concluded that although BA and BS resulted in similar mole% changes in the congener profiles, specific pathways were triggered with the applied treatment.

3.4. Microbial Community Composition and Diversity Shifts

Shotgun metagenomic sequencing revealed substantial shifts in the microbial community composition during the 198-day incubation. After quality filtering, 15.7 million high-quality reads were retained for the initial sediment, whereas 7.3, 3.1, and 5.5 million reads were retained for the BA, BS, and NA treatments, respectively, after 198 days of incubation.

Phylum-level community profiles are presented in Figure 3A, complemented by genus-level relative abundances in Table S7 and the accompanying heatmap in Figure S7. Pseudomonadota decreased from 76.81% in the initial sediment to 22.64%, 18.23%, and 21.03% in BA, BS, and NA, respectively, whereas Thermodesulfobacteriota, Actinomycetota, Bacillota, and Bacteroidota became more prominent (Figure 3A). Because broadly similar endpoint profiles were observed across BA, BS, and NA, prolonged anaerobic incubation appears to have been a major driver of overall community restructuring. Wang et al. [49] also observed nonmonotonic changes in diversity and a separation between the early and late-incubation communities during PBDE degradation.

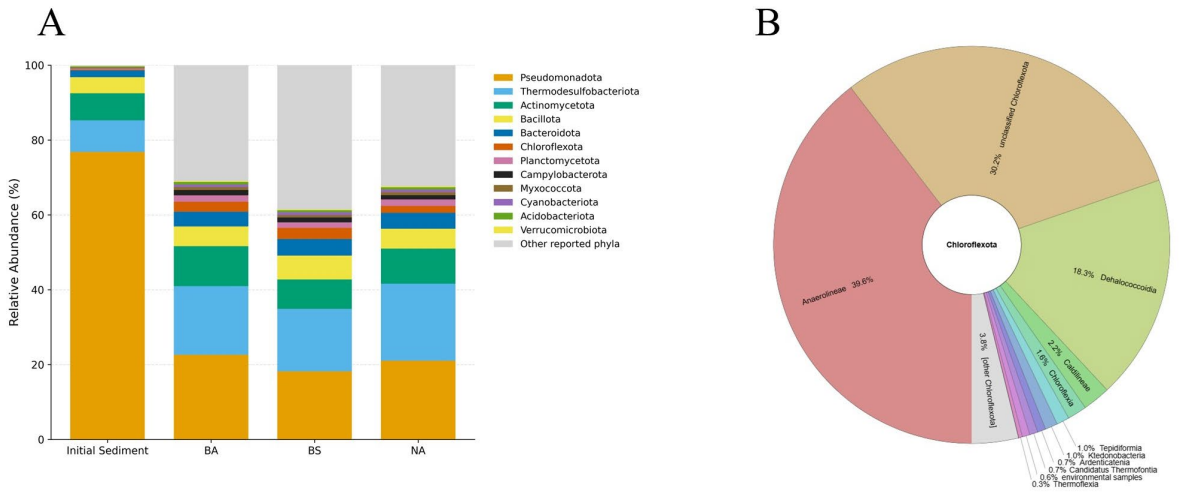


Figure 3. (**A**) Phylum-level community composition in the initial sediment and the day-198 bioaugmentation (BA), biostimulation (BS), and natural attenuation (NA) microcosms. Twelve selected bacterial phyla are shown individually, while the remaining phyla in the abundance tables are grouped as "Other reported phyla." Percentages are expressed relative to the complete reported phylum profile. (**B**) Krona visualization of the taxonomic composition of the Chloroflexota fraction in the BA microcosm at day 198.

The genus-level comparison revealed contrasting changes within individual phyla (Table S7 and Figure S7). Within Thermodesulfobacteriota, *Desulfobacter* and *Syntrophotalea* increased from 0.834% and 0.054% in the initial sediment to 4.930–5.787% and 3.773–5.014%, respectively, becoming the two most abundant genera in all three day-198 samples. In contrast, *Desulfosarcina* decreased from 5.759% to 1.361-1.787%. Within Actinomycetota, *Nocardioides* decreased from 12.950% to 0.235-0.339%, whereas *Streptomyces* decreased from 8.021% to 3.007-4.012% but remained the third most abundant genus in each endpoint sample. Other pronounced decreases included *Gimesia*, from 3.334% to 0.079-0.098%, and *Sulfurovum*, from 3.040% to 0.737-0.806%. These patterns illustrate changes within individual phyla that were not apparent from the phylum-level distributions alone.

Within Pseudomonadota, *Sulfitobacter* was initially more abundant than *Pseudomonas* (5.299% and 4.392%, respectively). By day 198, their relative abundances had decreased to 0.197-0.320% and 1.630-1.985%, respectively, leaving *Pseudomonas* as the most abundant genus within this phylum in all three treatments. Recent studies have demonstrated PCB- and PBDE-transforming capabilities in individual *Pseudomonas* strains. Yang et al.[50] reported that *Pseudomonas* sp. HR1 degraded 81.8% and 70.9% of Aroclor 1242 supplied at 1 and 5 mg/L, respectively, within 14 days in shaken cultures. More directly relevant to anaerobic conditions, Qi et al. [51] demonstrated that *Pseudomonas* sp. QS-1 transformed 12.4% of BDE-47 supplied at 0.5 mg/L within seven days under anaerobic conditions, compared with 47.5% under aerobic conditions. Anaerobic dehalogenation was supported by bromide release and the detection of lower-brominated congeners. These findings demonstrated relevant transformation capabilities in specific strains, but did not establish that the *Pseudomonas* populations detected in our microcosms possessed or expressed the same functions. Their direct contribution to PCB or PBDE transformation, the involvement of cometabolism, and potential indirect interactions with OHRB (such as fermentation, electron donor production, or trace oxygen scavenging) therefore remain unresolved.

Chloroflexota increased from 0.2% initially to 2.7%, 3.0%, and 1.8% of the day-198 communities in BA, BS, and NA, respectively (Figure 3A). Within this phylum, *Brevefilum* was more abundant in BA and BS (0.431% and 0.547%) than in NA (0.219%), with similar

treatment patterns observed for *Leptolinea* and *Pelolinea* (Table S7; Figure S7). These genera were not listed in the initial genus profile, preventing quantification of their changes from baseline. In contrast, *Dehalococcoides* remained at similarly low relative abundances: 0.0344% initially and 0.0313%, 0.0292%, and 0.0287% in BA, BS, and NA, respectively. A comparable lack of *Dehalococcoides* enrichment despite substantial PBDE degradation was reported by Zhu et al. [42], suggesting that organohalide-respiring populations may remain minor members of the sediment microbiome during contaminant transformation. The Chloroflexota fraction in BA also exhibited a heterogeneous taxonomic composition, dominated by Anaerolineae (40%) and unclassified Chloroflexota (30%), while Dehalococcoidia accounted for 18% of this fraction (Figure 3B). Thus, the abundance of Chloroflexota should not be interpreted as a direct indicator of *Dehalococcoides* enrichment or organohalide-respiring activity.

The low relative abundance of *Dehalococcoides* does not necessarily exclude a functional contribution. Xu et al. [29] demonstrated that defined *D. mccartyi* strains markedly enhanced penta-BDE dehalogenation while remaining minor components of the overall sediment community. However, that study used targeted qPCR and strain-specific functional markers, whereas the present comparison was based on relative metagenomic abundance within a complex microbial community. Consequently, changes in the absolute population size or metabolic activity of *Dehalococcoides* could not be resolved, and confirming its direct functional contribution would require targeted qPCR or functional gene (rdhA) expression analyses. The performance of the BA treatment might therefore reflect the collective activity of the site-derived consortium rather than enrichment of a single genus.

Alpha diversity also increased markedly over the 198-day incubation. The initial sediment had Shannon and Simpson (1-D) indices of 5.68 and 0.980, respectively, whereas Shannon values increased to 8.04, 7.93, and 8.00 in BA, BS, and NA, with corresponding Simpson values of approximately 0.996. These higher values indicated a more diverse and even community distribution after incubation. In contrast, differences among the three endpoint treatments were marginal, suggesting that the major increase in alpha diversity was common to all microcosms and was more closely associated with prolonged anaerobic incubation than with the treatment-specific effect. Wang et al. (2023) [49] likewise reported higher alpha diversity after prolonged anaerobic PBDE incubation. By contrast, Zhu et al. (2019) [42] reported a lower Shannon index in BDE-209-amended sediment than in the control, indicating that PBDE transformation can also proceed through selective enrichment of a narrower microbial subset. The observed increase in diversity, therefore, appears to reflect the specific characteristics of the weathered Aliağa sediment, mixed PCB-PBDE contamination, and long-term microcosm conditions.

The simultaneous presence of PCBs and PBDEs might also have influenced microbial interactions without producing a detectable increase in *Dehalococcoides*. Wang et al. (2021) [17] reported inhibition under combined PBDE exposure and attributed it to competition for shared dehalogenating populations, whereas Xu et al. (2024) [16] observed enhanced PCB and PBDE dehalogenation when multifunctional *Dehalococcoides* populations were present. These contrasting outcomes indicated that the effect of co-contamination depends strongly on consortium composition, the range of reductive dehalogenases present, contaminant bioavailability, and sediment conditions. Our findings were therefore likely governed by the functional capacity of the broader anaerobic consortium rather than by the abundance of a single taxon.

3.5. Ecological Risk Evaluation

Remediation aims to reduce the risk caused by contamination in the sediments. To evaluate whether the bioremediation strategies tested in this study could reduce

ecological risk, we computed RQs at each time point for PCB and PBDE congeners for which toxicity values have been reported. The ECOTOX database provides a wide range of toxicity values (NOEC, LOEC, LC50, etc.) for various species [23]. We restricted our search to fish species and saltwater, but since limited values were available for saltwater, we preferred to use all types of water tested for fish species.

The timely RQ changes for 11 PCB and 3 PBDE congeners in each bioremediation strategy are shown in Figure 4. As observed, most congeners remained in the low-to-minimal-risk region, while PCB-194, PCB-18, PCB-52, PCB-138, PCB-101, PCB-28, and PCB-1 were in the moderate-to-high-risk region. As dehalogenation proceeded, PCB-194's RQ decreased for BA and BS microcosms, whereas the NA microcosm showed an increase towards the end of incubation. Since PCB-194 is a high-Cl congener, its transformation was facilitated by the amendments, but without any intervention, its production might become more predominant than its transformation. At the end of 198 days, the risk posed by PCB-194 remained very high, indicating that long-term bioremediation strategies should be planned in the field. Other moderate-to-high-risk congeners, PCB-18 and PCB-52 are the products of dehalogenation, hence their RQs increased during bioremediation. Therefore, during the field application of bioremediation strategies, their further transformation should be favored. However, the end-products, i.e., mono-CBs, are expected to accumulate in an anaerobic system, hence their RQs increased in all sets. Although PCB-2 and -3 remained in the low-risk region in this study, PCB-1 was in the moderate-risk region throughout the incubation. Even though reductive dehalogenation decreases the environmental persistence and hydrophobicity of heavily halogenated parent congeners, lower halogenation does not inherently guarantee lower ecotoxicological risk. Toxicity and bioaccumulation depend strongly on congener-specific substitution patterns (e.g., molecular planarity), while higher aqueous solubility and bioavailability of dehalogenated intermediates can temporarily increase toxicological pressure on aquatic organisms[52–54]. Consequently, if complete detoxification is the aim, anaerobic dehalogenation should be coupled with aerobic degradation, in which less toxic products can be formed [55,56].

It is crucial to note that the RQ values were computed using the median of reported toxicity values, which might vary by orders of magnitude. For example, BDE-209 has 100 NOEC values, ranging from 10^{-5} to 200 mg/L (Table S3). Hence, the risk classification for BDE-209 might change depending on the NOEC value we used. This variation should be taken into account when evaluating the risk-reduction efficiency of the bioremediation strategy to be applied.

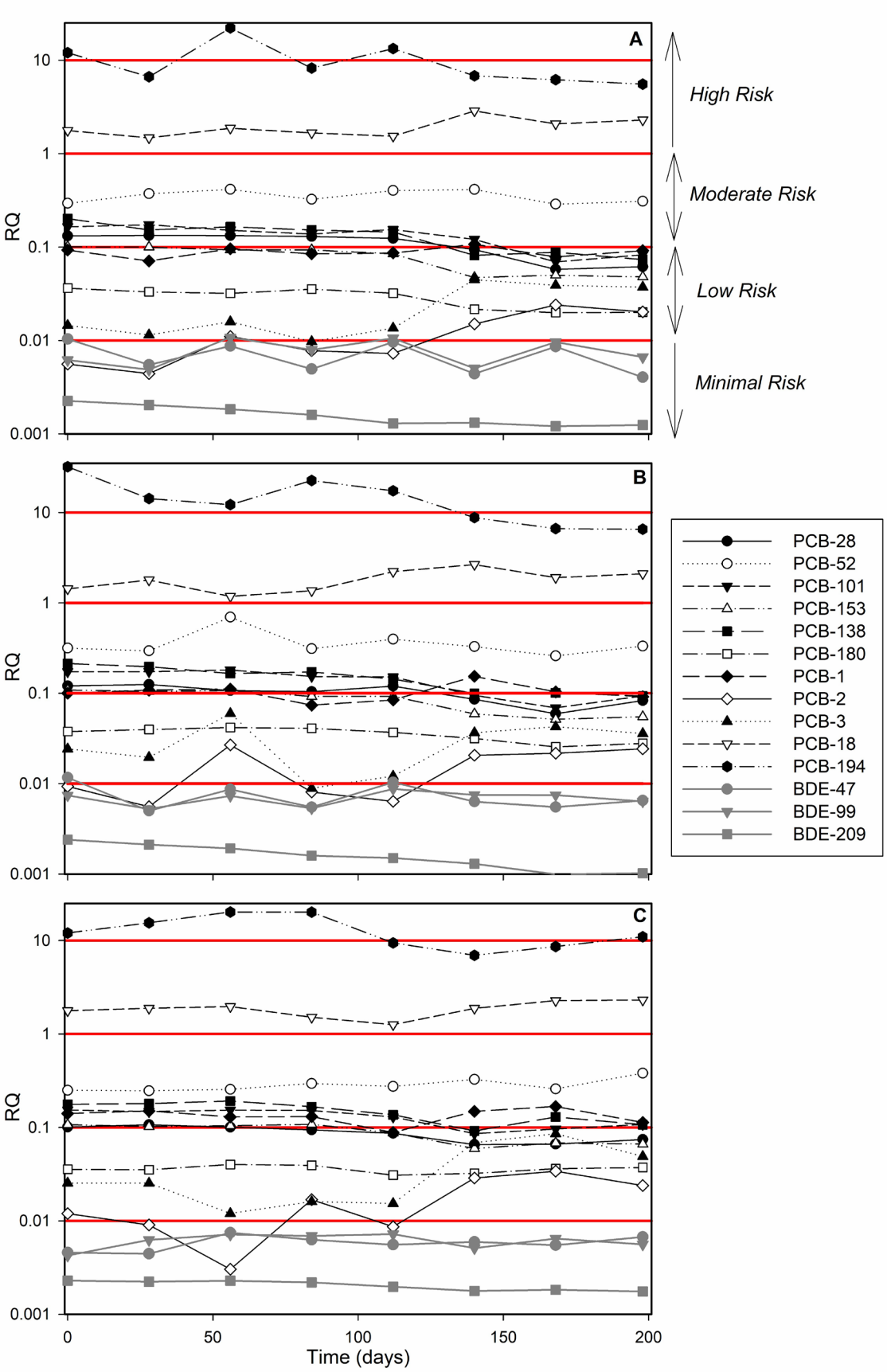


Figure 4. Time trends of risk quotients (RQ) for PCB and PBDE congeners in (**A**) bioaugmentation, (**B**) biostimulation, and (**C**) natural attenuation microcosms. Horizontal red lines represent the risk levels categorized as minimal (RQ < 0.01), low (0.01 ≤ RQ < 0.1), moderate (0.1 ≤ RQ < 1), and high (RQ ≥ 1) [24].

https://doi.org/10.3390/toxics14121070

4. Conclusions

This study provides comprehensive insights into the chemical, microbial, and ecotoxicological dynamics during the bioremediation of marine sediments chronically co-contaminated with weathered PCBs and PBDEs. Active bioremediation strategies significantly outperformed intrinsic natural attenuation. Overall, both biostimulation (utilizing acetate and essential micronutrients) and bioaugmentation (with the site-derived enrichment culture) achieved comparable remediation efficiency, yielding similar total mass removal and statistically indistinguishable dehalogenation rates. Consequently, in closed microcosms, the primary advantage of biostimulation lies in achieving comparable overall remediation performance by stimulating the indigenous microbial consortium without the added cost and operational complexity of cultivating and delivering exogenous anaerobic cultures. Across all microcosms, native halorespiring microorganisms exhibited a distinct preference for PBDEs over PCBs during early incubation. PBDEs underwent faster and more extensive dehalogenation, whereas PCB dehalogenation exhibited a longer lag phase, lower overall removal extent, and no statistically significant rate differences across treatments. This preferential utilization highlights that degradation kinetics in weathered field sediments deviate markedly from freshly spiked laboratory systems. The transition from a Pseudomonadota-dominated initial community to more diverse endpoint communities, together with the increased relative abundance of Chloroflexota, supported the development of anaerobic microbial populations with potential organohalide-transforming capacity. Tracking congener-level transformations underscored the importance of tailored strategies for treating mixed POP residues in sediments. Although active dehalogenation successfully transformed persistent highly halogenated parent compounds, it led to the transient accumulation of lower-halogenated, mobile, and toxic intermediates. Consequently, ecological risk evaluation indicated that standalone anaerobic dehalogenation may temporarily increase toxicological pressure in the marine ecosystem. For full-scale field implementation at heavily contaminated marine sediments, anaerobic bioremediation should be conceptualized as a primary treatment step. To achieve complete detoxification and "good environmental status" in the marine ecosystem, anaerobic dehalogenation must be integrated into a sequential treatment train (e.g., coupled anaerobic-aerobic zones or sediment capping with bio-amended reactive barriers) designed to mineralize accumulating lower-halogenated intermediates.

Supplementary Materials: The following supporting information can be downloaded at https://www.mdpi.com/article/10.3390/toxics14121070/s1, Figure S1: Mole percentages of PCB congeners analyzed in the water samples collected at day 198. Figure S2: Congener-specific mole percent differences between t = 0 and t = 198 day profiles for (A) PCBs and (B) PBDEs in bioaugmentation (BA) and biostimulation (BS) microcosms. Figure S3: Congener-specific temporal profiles for PCB dehalogenation in bioaugmentation microcosms. Figure S4: Congener-specific temporal profiles for PCB dehalogenation in biostimulation microcosms. Figure S5: Congener-specific temporal profiles for PBDE dehalogenation in bioaugmentation microcosms. Figure S6: Congener-specific temporal profiles for PBDE dehalogenation in biostimulation microcosms. Figure S7: Heatmap of genus-level relative abundances (%) in the initial sediment and the day-198 bioaugmentation (BA), biostimulation (BS), and natural attenuation (NA) microcosms. Table S1: Homolog group classification, quantifier/qualifier ions, method detection limits (MDLs), and limits of quantitation (LOQs) for the 46 targeted PCB congeners. Table S2: Homolog group classification, quantifier/qualifier ions, method detection limits (MDLs), and limits of quantitation (LOQs) for the 29 targeted PBDE congeners. Table S3: Components of artificial seawater medium (ASM) and artificial seawater (AS). Table S4: Toxicity values derived from ECOTOX database. The search was limited to fish species. Table S5: Total PCB molar mass balance in sediment microcosms with respect to day zero concentrations (%). * Day 198 mole balance involves the water-phase PCB concentrations. Table S6: Total PBDE

molar mass balance in sediment microcosms with respect to day zero concentrations (%). Table S7: Relative abundances (%) of selected bacterial genera in the initial sediment and the day-198 bioaugmentation (BA), biostimulation (BS), and natural attenuation (NA) microcosms.

Author Contributions: Conceptualization, H.D. and H.E.Ö.; methodology, H.D. and H.E.Ö.; validation, M.K., H.D. and H.E.Ö.; formal analysis, H.D.; investigation, M.K., H.D. and H.E.Ö.; resources, H.D. and H.E.Ö.; data curation, M.K. and H.D.; writing—original draft preparation, M.K.; writing—review and editing, H.D. and H.E.Ö.; visualization, M.K. and H.D.; supervision, H.D. and H.E.Ö.; project administration, H.D.; funding acquisition, H.D. All authors have read and agreed to the published version of the manuscript.

Funding: This research was funded by the Scientific and Technological Research Council of Türkiye (TUBITAK), grant number 122Y005, and Izmir Institute of Technology Coordination of Scientific Research Projects, grant number 2024IYTE-1-0038.

Institutional Review Board Statement: Not applicable.

Informed Consent Statement: Not applicable.

Data Availability Statement: The data presented in this study are available upon request from the corresponding author.

Acknowledgments: The authors would like to thank the Integrated Research Center of Izmir Institute of Technology for the GC-MS, TOC, and PCR analyses.

Conflicts of Interest: The authors declare no conflicts of interest.

Abbreviations

The following abbreviations are used in this manuscript:

AF	Assessment factor
ANOVA	Analysis of variance
AS	Artificial seawater
ASM	Artificial seawater medium
BA	Bioaugmentation
Br/dp/day	Bromine per diphenyl ether per day
BS	Biostimulation
Cl/bp/day	Chlorine per biphenyl per day
DF	Detection frequency
dw	Dry weight
f_{oc}	sediment organic-carbon fraction
EI	Electron impact ionization
GC-MS	Gas chromatography-mass spectrometry
K_{oc}	Sediment organic carbon-water distribution coefficients
LC50	Lethal concentration
LOEC	Lowest observed effect concentration
LOQ	Limit of quantitation
MDL	Method detection limit
MSD	Mass selective detector
NA	Natural attenuation
NC	Negative control
NOEC	No observed effect concentration
OHRB	Organohalide respiring bacteria
PBDE	Polybrominated diphenyl ether
PCB	Polychlorinated biphenyl
PNEC	Predicted no-effect concentration
POPs	Persistent organic pollutants
qPCR	Quantitative polymerase chain reaction
RQ	Risk quotient

SC	Sterile control
SIM	Selected ion monitoring
TOC	Total organic carbon
US EPA	United States Environmental Protection Agency

References

1. European Commission Marine Environment. EU Policies to Protect Europe's Oceans, Seas and Coasts. Available online: https://environment.ec.europa.eu/topics/marine-environment_en (accessed on 28 June 2026).
2. Neşer, G.; Kontas, A.; Ünsalan, D.; Altay, O.; Darilmaz, E.; Uluturhan, E.; Küçüksezgin, F.; Tekoğul, N.; Yercan, F. Polycyclic Aromatic and Aliphatic Hydrocarbons Pollution at the Coast of Aliağa (Turkey) Ship Recycling Zone. *Mar. Pollut. Bull.* **2012**, *64*, 1055–1059. https://doi.org/10.1016/j.marpolbul.2012.02.019.
3. Pazi, I.; Kucuksezgin, F.; Tolga Gonul, L. Occurrence and Distribution of Organochlorine Residues in Surface Sediments of the Candarli Gulf (Eastern Aegean). *Mar. Pollut. Bull.* **2012**, *64*, 2839–2843. https://doi.org/10.1016/j.marpolbul.2012.09.008.
4. Odabasi, M.; Dumanoglu, Y.; Kara, M.; Altiok, H.; Elbir, T.; Bayram, A. Spatial Variation of PAHs and PCBs in Coastal Air, Seawater, and Sediments in a Heavily Industrialized Region. *Environ. Sci. Pollut. Res.* **2017**, *24*, 13749–13759. https://doi.org/10.1007/s11356-017-8991-8.
5. Yılmaz, A.; Karacık, B.; Yakan, S.D.; Henkelmann, B.; Schramm, K.W.; Okay, O.S. Organic and Heavy Metal Pollution in Shipbreaking Yards. *Ocean Eng.* **2016**, *123*, 452–457. https://doi.org/10.1016/j.oceaneng.2016.06.036.
6. Muzyed, S.K.I.; Kucuksezgin, F.; Tuzmen, N. Persistent Organochlorine Residues in Fish and Sediments Collected from Eastern Aegean Coast: Levels, Occurrence and Ecological Risk. *Mar. Pollut. Bull.* **2017**, *119*, 247–252. https://doi.org/10.1016/j.marpolbul.2017.04.040.
7. Demirtepe, H. Surface Sediments as a Sink and Risk Source for Legacy POPs during Waste Management Practices. *Environ. Pollut.* **2025**, *373*, 126128. https://doi.org/10.1016/j.envpol.2025.126128.
8. Seidel, K.; Kühnert, J.; Adrian, L. The Complexome of *Dehalococcoides mccartyi* Reveals Its Organohalide Respiration-Complex Is Modular. *Front. Microbiol.* **2018**, *9*, 1130. https://doi.org/10.3389/fmicb.2018.01130.
9. Dang, H.; Ewald, J.M.; Mattes, T.E. Genome-Resolved Metagenomics and Metatranscriptomics Reveal Insights into the Ecology and Metabolism of Anaerobic Microbial Communities in PCB-Contaminated Sediments. *Environ. Sci. Technol.* **2023**, *57*, 16386–16398. https://doi.org/10.1021/acs.est.3c05439.
10. Zhang, Z.; Li, Z.; Nan, J.; Ouyang, J.; Chen, X.; Wang, H.; Wang, A. Evaluating Advancements and Opportunities in Electro-Assisted Biodehalogenation of Emerging Halogenated Contaminants. *Bioresour. Technol.* **2025**, *419*, 132011. https://doi.org/10.1016/j.biortech.2024.132011.
11. Payne, R.B.; May, H.D.; Sowers, K.R. Enhanced Reductive Dechlorination of Polychlorinated Biphenyl Impacted Sediment by Bioaugmentation with a Dehalorespiring Bacterium. *Environ. Sci. Technol.* **2011**, *45*, 8772–8779.
12. Matturro, B.; Ubaldi, C.; Grenni, P.; Caracciolo, A.B.; Rossetti, S. Polychlorinated Biphenyl (PCB) Anaerobic Degradation in Marine Sediments: Microcosm Study and Role of Autochthonous Microbial Communities. *Environ. Sci. Pollut. Res.* **2016**, *23*, 12613–12623. https://doi.org/10.1007/s11356-015-4960-2.
13. Pan, Y.; Chen, J.; Zhou, H.; Cheung, S.G.; Tam, N.F.Y. Degradation of BDE-47 in Mangrove Sediments with Amendment of Extra Carbon Sources. *Mar. Pollut. Bull.* **2020**, *153*, 110972. https://doi.org/10.1016/j.marpolbul.2020.110972.
14. Qiu, M.; Chen, X.; Deng, D.; Guo, J.; Sun, G.; Mai, B.; Xu, M. Effects of Electron Donors on Anaerobic Microbial Debromination of Polybrominated Diphenyl Ethers (PBDEs). *Biodegradation* **2012**, *23*, 351–361. https://doi.org/10.1007/s10532-011-9514-9.
15. Demirtepe, H.; Imamoglu, I. Degradation of Decabromodiphenyl Ether (BDE-209) in Microcosms Mimicking Sediment Environment Subjected to Comparative Bioremediation Strategies. *J. Environ. Manag.* **2019**, *233*, 120–130. https://doi.org/10.1016/j.jenvman.2018.11.144.
16. Xu, G.; Ng, H.L.; Chen, C.; Rogers, M.J.; He, J. Combatting Multiple Aromatic Organohalide Pollutants in Sediments by Bioaugmentation with a Single *Dehalococcoides*. *Water Res.* **2024**, *255*, 121447. https://doi.org/10.1016/j.watres.2024.121447.
17. Wang, G.; Jiang, N.; Liu, Y.; Wang, X.; Liu, Y.; Jiao, D.; Wang, H. Competitive Microbial Degradation among PBDE Congeners in Anaerobic Wetland Sediments: Implication by Multiple-Line Evidences Including Compound-Specific Stable Isotope Analysis. *J. Hazard. Mater.* **2021**, *412*, 125233. https://doi.org/10.1016/j.jhazmat.2021.125233.
18. Berges, J.A.; Franklin, D.J.; Harrison, P.J. Evolution of an Artificial Seawater Medium: Improvements in Enriched Seawater, Artificial Water over the Last Two Decades. *J. Phycol.* **2001**, *37*, 1138–1145. https://doi.org/10.1046/j.1529-8817.2001.01052.x.

19. Wolin, E.A.; Wolin, M.J.; Wolfe, R.S. Formation of Methane by Bacterial Extracts. *J. Biol. Chem.* **1963**, *238*, 2882–2886. https://doi.org/10.1016/s0021-9258(18)67912-8.
20. U.S. Environmental Protection Agency (USEPA). *Method 3665A Sulfuric Acid/Permanganate Cleanup*; U.S. Environmental Protection Agency (USEPA): Washington, DC, USA, 1996.
21. Abramowicz, D.A.; Brennan, M.J.; Van Dort, H.M.; Gallagher, E.L. Factors Influencing the Rate of Polychlorinated Biphenyl Dechlorination in Hudson River Sediments. *Environ. Sci. Technol.* **1993**, *27*, 1125–1131.
22. Chen, Y.; Tan, Y.; Feng, Y.; Dong, T.; Jiang, C.; Wang, C.; Yang, Y.; Zhang, Z. Selected Legacy and Emerging Organic Contaminants in Sediments of China's Yangtze—The World's Third Longest River: Response to Anthropogenic Activities. *Environ. Pollut.* **2024**, *346*, 123608. https://doi.org/10.1016/j.envpol.2024.123608.
23. USEPA. ECOTOX Knowledgebase. Available online: https://cfpub.epa.gov/ecotox/ (accessed on 4 August 2026).
24. European Commission. *Technical Guidance Document on Risk Assessment in Support of Commission Directive 93/67/EEC on Risk Assessment for New Notified Substances, Commission Regulation (EC) No 1488/94 on Risk Assessment for Existing Substances, Directive 98/8/EC of the European Parliament and of the Council Concerning the Placing of Biocidal Products on the Market*, 2nd ed.; Office for Official Publications of the European Communities: Luxembourg, 2003.
25. Xu, L.; Tang, Y.; Liu, S.; Chen, X.; Wang, Y.; Liu, Z.; Qin, Q.; Fu, D.; Xu, Y. Short-Chain Fatty Acids Facilitated Long-Term Dechlorination of PCBs in Taihu Lake Sediment Microcosms: Evidence from PCB Congener and Microbial Community Analyses. *Chemosphere* **2023**, *340*, 139935. https://doi.org/10.1016/j.chemosphere.2023.139935.
26. Alonso, F.; Beletskaya, I.P.; Yus, M. Metal-Mediated Reductive Hydrodehalogenation of Organic Halides. *Chem. Rev.* **2002**, *102*, 4009–4091. https://doi.org/10.1021/cr0102967.
27. Zeng, X.; Massey Simonich, S.L.; Robrock, K.R.; Korytár, P.; Alvarez-Cohen, L.; Barofsky, D.F. Application of a Congener-Specific Debromination Model to Study Photodebromination, Anaerobic Microbial Debromination, and FE0 Reduction of Polybrominated Diphenyl Ethers. *Environ. Toxicol. Chem.* **2010**, *29*, 770–778. https://doi.org/10.1002/etc.119.
28. Robrock, K.R.; Korytár, P.; Alvarez-Cohen, L. Pathways for the Anaerobic Microbial Debromination of Polybrominated Diphenyl Ethers. *Environ. Sci. Technol.* **2008**, *42*, 2845–2852.
29. Xu, G.; Ng, H.L.; Chen, C.; Zhao, S.; He, J. Efficient and Complete Detoxification of Polybrominated Diphenyl Ethers in Sediments Achieved by Bioaugmentation with Dehalococcoides and Microbial Ecological Insights. *Environ. Sci. Technol.* **2022**, *56*, 8008–8019. https://doi.org/10.1021/acs.est.2c00914.
30. Desforges, J.P.W.; Dangerfield, N.; Shaw, P.D.; Ross, P.S. Heightened Biological Uptake of Polybrominated Diphenyl Ethers Relative to Polychlorinated Biphenyls Near-Source Revealed by Sediment and Plankton Profiles along a Coastal Transect in British Columbia. *Environ. Sci. Technol.* **2014**, *48*, 6981–6988. https://doi.org/10.1021/es500218b.
31. Magar, V.S.; Brenner, R.C.; Johnson, G.W.; Quensen, J.F. Long-Term Recovery of PCB-Contaminated Sediments at the Lake Hartwell Superfund Site: PCB Dechlorination. 2. Rates and Extent. *Environ. Sci. Technol.* **2005**, *39*, 3548–3554.
32. Demirtepe, H.; Kjellerup, B.; Sowers, K.R.; Imamoglu, I. Evaluation of PCB Dechlorination Pathways in Anaerobic Sediment Microcosms Using an Anaerobic Dechlorination Model. *J. Hazard. Mater.* **2015**, *296*, 120–127. https://doi.org/10.1016/j.jhazmat.2015.04.033.
33. Kjellerup, B.V.; Naff, C.; Edwards, S.J.; Ghosh, U.; Baker, J.E.; Sowers, K.R. Effects of Activated Carbon on Reductive Dechlorination of PCBs by Organohalide Respiring Bacteria Indigenous to Sediments. *Water Res.* **2014**, *52*, 1–10. https://doi.org/10.1016/j.watres.2013.12.030.
34. Fagervold, S.K.; Watts, J.E.M.; May, H.D.; Sowers, K.R. Effects of Bioaugmentation on Indigenous PCB Dechlorinating Activity in Sediment Microcosms. *Water Res.* **2011**, *45*, 3899–3907. https://doi.org/10.1016/j.watres.2011.04.048.
35. Löffler, F.E.; Yan, J.; Ritalahti, K.M.; Adrian, L.; Edwards, E.A.; Konstantinidis, K.T.; Müller, J.A.; Fullerton, H.; Zinder, S.H.; Spormann, A.M. *Dehalococcoides mccartyi* gen. nov., sp. nov., obligately organohalide-respiring anaerobic bacteria relevant to halogen cycling and bioremediation, belong to a novel bacterial class, *Dehalococcoidia* classis nov., order *Dehalococcoidales* ord. nov. and family *Dehalococcoidaceae* fam. nov., within the phylum *Chloroflexi*. *Int. J. Syst. Evol. Microbiol.* **2013**, *63*, 625–635. https://doi.org/10.1099/ijs.0.034926-0.
36. Fennell, D.E.; Gossett, J.M.; Zinder, S.H. Comparison of Butyric Acid, Ethanol, Lactic Acid, and Propionic Acid as Hydrogen Donors for the Reductive Dechlorination of Tetrachloroethene. *Environ. Sci. Technol.* **1997**, *31*, 918–926. https://doi.org/10.1021/es960756r.

37. Hattori, S. Syntrophic Acetate-Oxidizing Microbes in Methanogenic Environments. *Microbes Environ.* **2008**, *23*, 118–127. https://doi.org/10.1264/jsme2.23.118.
38. Hug, L.A.; Beiko, R.G.; Rowe, A.R.; Richardson, R.E.; Edwards, E.A. Comparative Metagenomics of Three Dehalococcoides-Containing Enrichment Cultures: The Role of the Non-Dechlorinating Community. *BMC Genom.* **2012**, *13*, 327. https://doi.org/10.1186/1471-2164-13-327.
39. Tokarz, J.A., III; Ahn, M.-Y.; Leng, J.; Filley, T.R.; Nies, L. Reductive Debromination of Polybrominated Diphenyl Ethers in Anaerobic Sediment and a Biomimetic System. *Environ. Sci. Technol.* **2008**, *42*, 1157–1164.
40. Huang, H.W.; Chang, B.V.; Lee, C.C. Reductive Debromination of Decabromodiphenyl Ether by Anaerobic Microbes from River Sediment. *Int. Biodeterior. Biodegrad.* **2014**, *87*, 60–65. https://doi.org/10.1016/j.ibiod.2013.10.011.
41. Xu, G.; Lu, Q.; Yu, L.; Wang, S. Tetrachloroethene Primes Reductive Dechlorination of Polychlorinated Biphenyls in a River Sediment Microcosm. *Water Res.* **2019**, *152*, 87–95. https://doi.org/10.1016/j.watres.2018.12.061.
42. Zhu, X.; Zhong, Y.; Wang, H.; Li, D.; Deng, Y.; Peng, P. New Insights into the Anaerobic Microbial Degradation of Decabrominated Diphenyl Ether (BDE-209) in Coastal Marine Sediments. *Environ. Pollut.* **2019**, *255*, 113151. https://doi.org/10.1016/j.envpol.2019.113151.
43. Gerecke, A.C.; Giger, W.; Hartmann, P.C.; Heeb, N.V.; Kohler, H.-P.E.; Schmid, P.; Zennegg, M.; Kohler, M. Anaerobic Degradation of Brominated Flame Retardants in Sewage Sludge. *Chemosphere* **2006**, *64*, 311–317. https://doi.org/10.1016/j.chemosphere.2005.12.016.
44. Zhang, C.; Katayama, A. Humin as an Electron Mediator for Microbial Reductive Dehalogenation. *Environ. Sci. Technol.* **2012**, *46*, 6575–6583. https://doi.org/10.1021/es3002025.
45. Zhang, Z.; Liu, X.; Li, Z.; Chen, X.; Zu, Y.; Ho, S.H.; Liang, B.; Zhou, S.; Wang, A. Humin Oxidation Drives Microbial Dehalogenation in Oligotrophic Environments. *ISME J.* **2025**, *19*, wraf207. https://doi.org/10.1093/ismejo/wraf207.
46. Xu, L.; Liu, S.; Tang, Y.; Han, X.; Wang, Y.; Fu, D.; Qin, Q.; Xu, Y. Long-Term Dechlorination of Polychlorinated Biphenyls (PCBs) in Taihu Lake Sediment Microcosms: Identification of New Pathways, PCB-Driven Shifts of Microbial Communities, and Insights into Dechlorination Potential. *Environ. Sci. Technol.* **2022**, *56*, 938–950. https://doi.org/10.1021/acs.est.1c06057.
47. Orihel, D.M.; Bisbicos, T.; Darling, C.T.R.; Dupuis, A.P.; Williamson, M.; Muir, D.C.G. Probing the Debromination of the Flame Retardant Decabromodiphenyl Ether in Sediments of a Boreal Lake. *Environ. Toxicol. Chem.* **2016**, *35*, 573–583. https://doi.org/10.1002/etc.3229.
48. Gerecke, A.C.; Hartmann, P.C.; Heeb, N.V.; Kohler, H.-P.E.; Giger, W.; Schmid, P.; Zennegg, M.; Kohler, M. Anaerobic Degradation of Decabromodiphenyl Ether. *Environ. Sci. Technol.* **2005**, *39*, 1078–1083.
49. Wang, X.; Wang, G.; Li, C.; Liu, Y.; Jiang, N.; Dong, X.; Wang, H. Systematic Characterization of Sediment Microbial Community Structure and Function Associated with Anaerobic Microbial Degradation of PBDEs in Coastal Wetland. *Mar. Pollut. Bull.* **2023**, *188*, 114622. https://doi.org/10.1016/j.marpolbul.2023.114622.
50. Yang, Y.; Zhang, Q.; Lin, Q.; Sun, F.; Shen, C.; Lin, H.; Su, X. Unveiling the PCB Biodegradation Potential and Stress Survival Strategies of Resuscitated Strain Pseudomonas Sp. HR1. *Environ. Pollut.* **2024**, *344*, 123320. https://doi.org/10.1016/j.envpol.2024.123320.
51. Qi, X.; Wang, Z.; Xia, Q.; Liang, X.; Wang, G.; Xu, C.; Lv, G.; Cai, J.; Cheng, Z.; Yang, Z.; et al. Aerobic and Anaerobic Degradation of BDE-47 by Facultative Anaerobe Pseudomonas Sp. QS-1: Pathway, Product Toxicity, and Bio-Augmentation Remediation. *Process Saf. Environ. Prot.* **2026**, *213*, 109014. https://doi.org/10.1016/j.psep.2026.109014.
52. DeVito, M.; Bokkers, B.; van Duursen, M.B.M.; van Ede, K.; Feeley, M.; Antunes Fernandes Gáspár, E.; Haws, L.; Kennedy, S.; Peterson, R.E.; Hoogenboom, R.; et al. The 2022 World Health Organization Reevaluation of Human and Mammalian Toxic Equivalency Factors for Polychlorinated Dioxins, Dibenzofurans and Biphenyls. *Regul. Toxicol. Pharmacol.* **2024**, *146*, 105525. https://doi.org/10.1016/j.yrtph.2023.105525.
53. Ciparis, S.; Hale, R.C. Bioavailability of Polybrominated Diphenyl Ether Flame Retardants in Biosolids and Spiked Sediment to the Aquatic Oligochaete, Lumbriculus Variegatus. *Environ. Toxicol. Chem.* **2005**, *24*, 916–925. https://doi.org/10.1897/04-179R.1.
54. Kuo, Y.M.; Sepúlveda, M.S.; Hua, I.; Ochoa-Acuña, H.G.; Sutton, T.M. Bioaccumulation and Biomagnification of Polybrominated Diphenyl Ethers in a Food Web of Lake Michigan. *Ecotoxicology* **2010**, *19*, 623–634. https://doi.org/10.1007/s10646-009-0431-1.

55. Pan, Y.; Chen, J.; Zhou, H.; Cheung, S.G.; Tam, N.F.Y. Degradation of BDE-47 in Mangrove Sediments under Alternating Anaerobic-Aerobic Conditions. *J. Hazard. Mater.* **2019**, *378*, 120709. https://doi.org/10.1016/j.jhazmat.2019.05.102.
56. Payne, R.B.; Ghosh, U.; May, H.D.; Marshall, C.W.; Sowers, K.R. A Pilot-Scale Field Study: In Situ Treatment of PCB-Impacted Sediments with Bioamended Activated Carbon. *Environ. Sci. Technol.* **2019**, *53*, 2626–2634. https://doi.org/10.1021/acs.est.8b05019.

Disclaimer/Publisher's Note: The statements, opinions and data contained in all publications are solely those of the individual author(s) and contributor(s) and not of MDPI and/or the editor(s). MDPI and/or the editor(s) disclaim responsibility for any injury to people or property resulting from any ideas, methods, instructions or products referred to in the content.